Promega

# Flexible Nucleic Acid Solutions

## for forensic laboratories

With preloaded methods for sample preprocessing and post-purification applications, the Maxwell® RSC 48 Instrument and the Maxprep™ Liquid Handler easily integrate into your laboratory workflow. There are no methods to create or protocols to write—the instruments are ready to do the tedious work for you.

- **Flexible:** Process 1 to 48 samples.
- **Reliable:** Consistent yields of high-quality DNA from casework samples.
- **Intuitive Software:** Preprogrammed protocols get you up and running quickly.

Personal Automation for the Forensic Lab

**www.promega.com/MaxprepForensics**

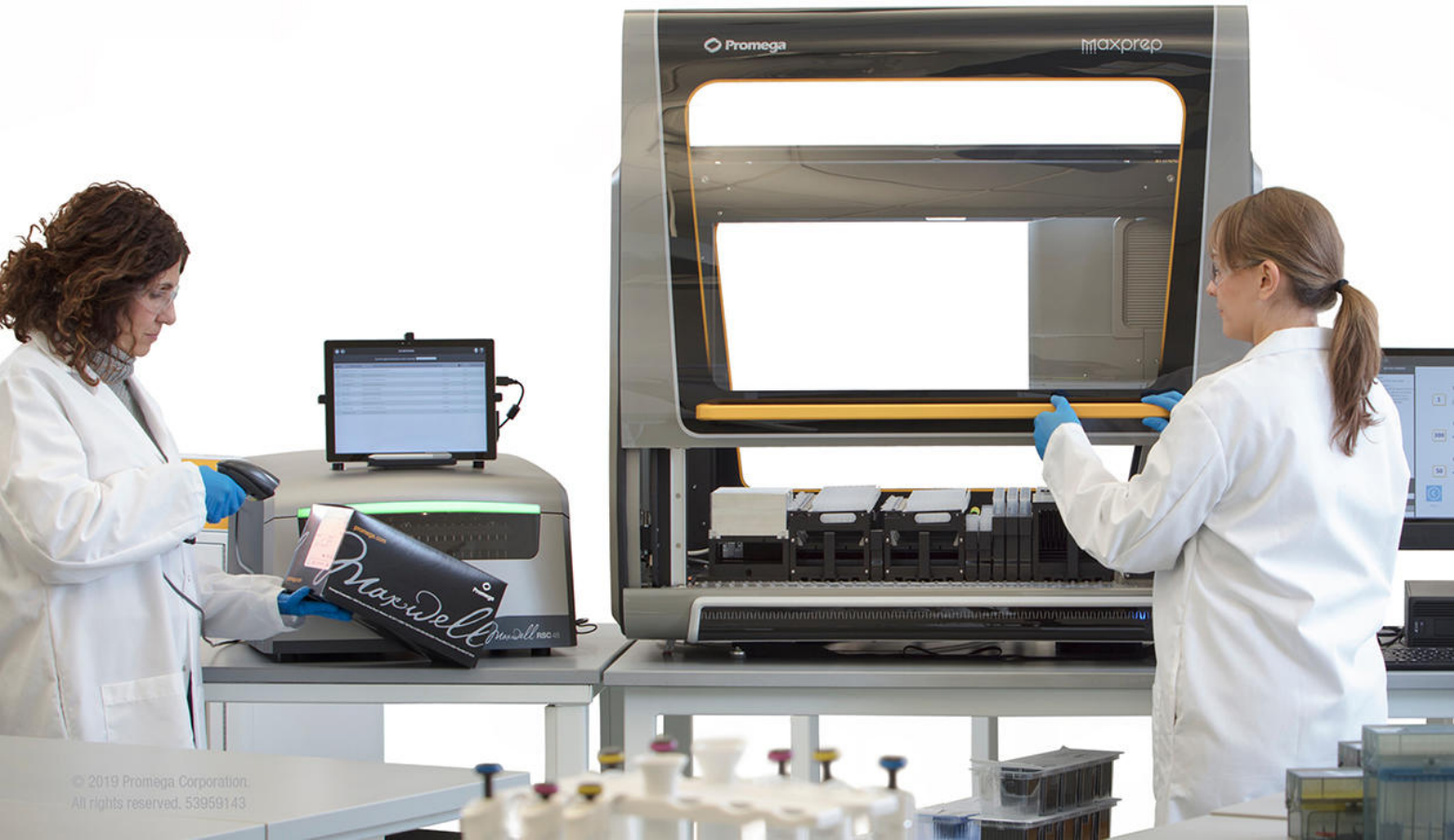

JOURNAL OF FORENSIC SCIENCES

*J Forensic Sci*, May 2013, Vol. 58, No. 3
doi: 10.1111/1556-4029.12094
Available online at: onlinelibrary.wiley.com

**PAPER**

**PATHOLOGY/BIOLOGY; ANTHROPOLOGY; ENGINEERING SCIENCES**

*Brian J. Powell,*[1] *M.S.; Nicholas V. Passalacqua,*[2] *Ph.D.; Todd W. Fenton,*[2] *Ph.D.; and Roger C. Haut,*[1] *Ph.D.*

# Fracture Characteristics of Entrapped Head Impacts Versus Controlled Head Drops in Infant Porcine Specimens*,†,‡

**ABSTRACT:** In many forensic cases, the job of forensic pathologists and anthropologists is to determine whether pediatric death is due to an abusive act or an accidental fall. The goal of this study was to compare the cranial fracture patterns generated on the parietal bone of a developing, infant porcine (pig, *Sus scrofa*) model by a controlled energy head drop onto a plate versus previous data generated by blunt force impact at the same energy onto the head constrained to a plate. The results showed that blunt force impacts on a head constrained to a rigid plate produces more fracture, but the same general pattern, as that for a head dropped onto the plate with the same level of impact energy. The study suggests that head constraint may be an important factor to consider in the evaluation of death causation for blunt force impacts to the pediatric skull.

**KEYWORDS:** forensic science, skull fracture, infant, porcine, energy dependency, interface dependency, age dependency, Geographic Information Systems

Traumatic injury to the head is a leading cause of death in infant humans (1). Head injuries have been shown to account for 80% of fatal child abuse in young children (2). On the other hand, children often sustain head trauma from accidental falls during development of walking motor skills or from child support devices such as high chairs (3,4). Falls, in fact, are the third leading cause of death in infants aged 1–4 years (5). Furthermore, "falls are the most common type of accident in young children as well as the most common history provided by caretakers suspected of child abuse" (6, p. 321). In many forensic cases, it is the job of forensic pathologists and forensic anthropologists to determine whether a pediatric death is due to an abusive act or an accidental fall. The most commonly fractured cranial bone in accidental and abuse cases is the parietal (7–9), and the current literature describes linear, complex, and depressed fractures for both types of cases (10–12). In several early studies, for example, it has been suggested that a number of specific characteristics of cranial fracture, including multiple bone fractures and those that cross sutures, are more frequent in abuse than in accidental injury cases. And yet, the results of early hallmark studies by Weber (13,14), where infant cadavers were dropped occiput-first onto different surfaces from 0.8 m, show multiple fractures around the cranium that often appeared to cross sutures. In simulation studies of the Weber experiments, using an instrumented anthropomorphic dummy, Coats and Margulies (6) estimated the forces that produce linear fractures on the infant cadaver skull in these experiments to be in the range of 930–1600 N. The lack of sufficient scientific data from controlled experimental studies in the literature on cranial fracture mechanics still poses a significant challenge to medico-legal professionals in correctly diagnosing skull fracture as being due to abuse or an accidental fall.

Case-based investigations of suspected child abuse (15) and falls (16) are often used in injury biomechanics studies. Some investigators use animal models to help understand mechanisms of injury, such as for cranial (17) and long bone (18) fractures. A porcine head model has recently been utilized in our laboratory to investigate some of the effects of contact interface and impact energy on cranial fracture patterns as a function of infant age (1,19). Justification for using this model has been provided in the previous studies by Baumer et al. (19,20). In the latter study, the authors also showed that age-related mechanical properties of the developing infant porcine parietal bone under bending loads parallel with those from human infant specimens. The studies of Baumer et al. (19) and Powell et al. (21) have entrapped the porcine head in a bed of epoxy to help prevent motion and impacted the parietal bone with deformable or rigid impact interfaces (Fig. 1). This experimental setting was used as an experimental method to simulate those forensic cases in which the head may be constrained, such as when it is impacted while lying against an asphalt or cement surface (22). In low-impact energy studies, cranial fractures on this model initiate at bone–suture boundaries remote from the site of impact at the center of the parietal bone (19). The study also indicates relatively more cranial fractures for a given level of impact

[1]Orthopaedic Biomechanics Laboratories, College of Osteopathic Medicine, Michigan State University, East Lansing, MI 48824.
[2]Department of Anthropology, College of Social Sciences, Michigan State University, East Lansing, MI 48824.

*Presented in part at the 64th Annual Scientific Meeting of the American Academic of Forensic Sciences, February 20–25, 2012, in Atlanta, GA.
†Funded by the National Institute of Justice, Office of Justice Programs, United States Department of Justice (2007-DN-BX-K196).
‡The opinions, findings, and conclusions expressed in this publication are those of the authors and do not necessarily reflect the views of the Department of Justice.

Received 27 Sept. 2011; and in revised form 16 Jan. 2012; accepted 25 Mar. 2012.

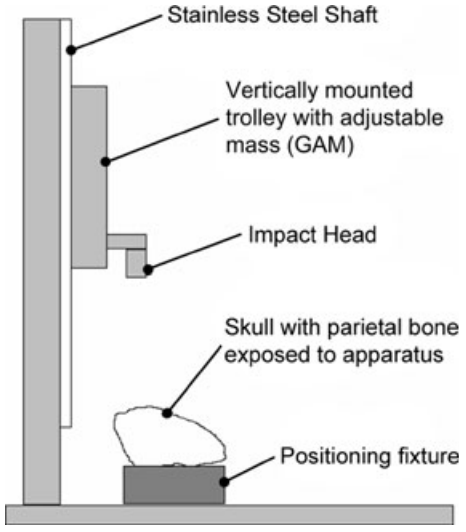


FIG. 1—*Setup of entrapped drop test fixture (21).*

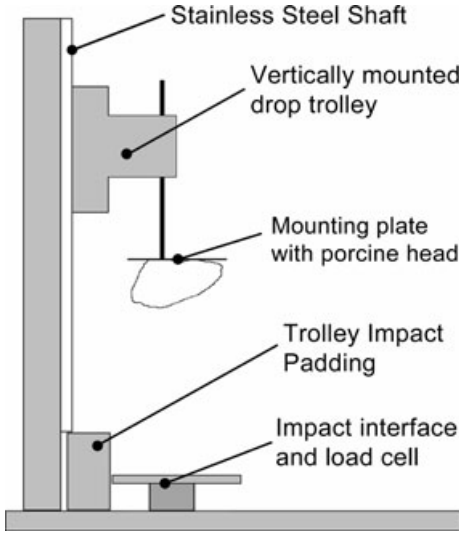


FIG. 2—*Schematic of free-fall drop tower.*

energy using a deformable contact interface than a rigid interface for specimens aged less than approximately 17 days. Baumer et al. (20) also show higher mechanical stiffness of bone–suture–bone cranial beam specimens from animals aged 18–21 days than for those less than 14 days of age. In this younger group, there is also greater suture stiffness in specimens older than 10 days of age. More recent studies by Powell et al. (21) demonstrate that when the impact energy level is doubled, cranial fractures often extend across suture boundaries and into adjacent cranial bones. Chason et al. (23) have also previously impacted canine heads that were both fixed and free to rotate and show higher intracranial pressures with increased susceptibility to concussion when the head is fixed. But, the effects of head restraint on the degree and patterns of cranial fracture are still lacking in the current literature for either human cadaver specimens or animal models. In this study, porcine heads were dropped in free fall with the same impact energy as in Powell et al. (21) to compare the degree and pattern of skull fracture with previous studies on the constrained head. These data may help provide more biomechanical information to better understand the role of head constraint in the patterns of fracture from cranial blunt impacts. Ultimately, these data may help guide the analysis of case studies on the human victim, as forensic pathologists and forensic anthropologists attempt to establish causality in cases of accidental and abusive pediatric death.

## Materials and Methods

A total of 31 porcine specimens were received from a farm and stored at a temperature of −20°C. All animals died of natural causes and were frozen within 12 h of death. The specimens ranged from 2–17 days of age. The specimens were thawed at room temperature for ~24 h before the tests. Each animal was inspected for initial head injury by palpating the parietal bone prior to experimentation.

Each specimen was fastened to a mounting plate using Velcro straps. A ball and socket clamp was fastened to a mounting plate and used to orient the parietal bone normal to the impact interface. The mounting plate was then attached to a hollow aluminum rod on which a gravity accelerated trolley was attached (Fig. 2). The trolley could be clamped to the rod at any

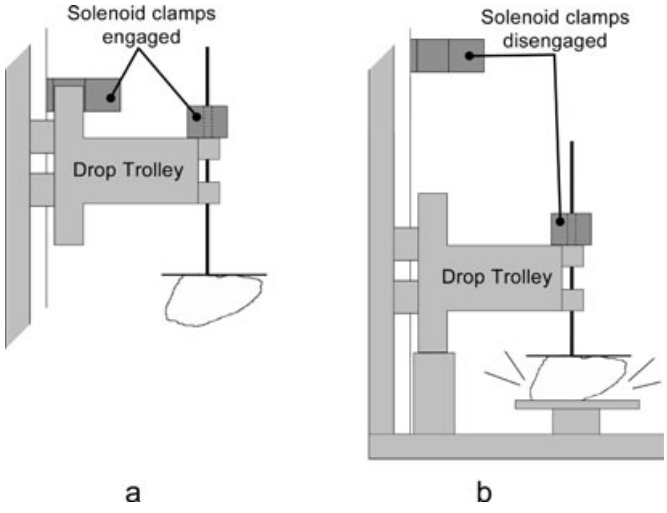


FIG. 3—*The drop trolley was raised to the necessary drop height and held with the electromagnetic solenoid clamp (a). The free-fall impact was produced by disengaging the solenoid clamps (b). The mounting rod was free to move vertically until the impact force returned to zero.*

time by activation of an electromagnetic solenoid, acting as a catch-and-release mechanism (Fig. 3).

To produce the necessary impact energy, the trolley was raised to the necessary drop height and held in place by a second electromagnetic solenoid (Fig. 3). The solenoid was fastened to a crossbar to adjust the drop height to a maximum of 9 feet. During the experiment, both solenoids disengaged, allowing the trolley and mounting plate with the head to fall freely. Upon impact, the trolley base struck a soft-padded surface to dissipate its drop energy. The skull impacted a rigid, aluminum interface. A load transducer (2.22 kN capacity, model 1010AF-500; Interface, Scottsdale, AZ) mounted immediately behind the impact interface recorded the impact force. The skull was allowed to impact only once using an operational amplifier comparator circuit to monitor the impact and re-energize the electromagnetic solenoid to catch the rod immediately after the impact force returned to zero. The force data were sampled at 10,000 Hz.

The impact energy levels for various aged specimens in this study were matched with those energy levels of the previous experiments by Powell et al. (21). These levels produced cranial fractures in the constrained head experiments. The height from which each head was dropped was determined using the expression

$$U = m * g * h$$

where $U$ was the potential impact energy, $m$ was the mass of each head (cut at the first cervical vertebrae), $g$ was the gravitational acceleration, and $h$ was the respective drop height needed to match the input energy levels of Powell et al. (21). In those experiments, the porcine heads were laid in a bed of room temperature curing epoxy resin (FibreStrand; Martin Senour Corp., Cleveland, OH) with the parietal bone oriented perpendicular to a dropped mass with a rigid impact interface, as described in detail in Powell et al. (21). Briefly, the impact energies used in Powell et al. (21) were twice the levels shown to initiate fracture at each age in this porcine model, as determined in a previous study by our laboratory (19). The impact interface was a solid aluminum cylinder with approximately 16 $cm^2$ of surface area. Impact energy was controlled by varying the drop height of a 1.67-kg mass. The impact mass (trolley) rode on the previously described guide rod, and it was arrested after a single impact to the center of the right parietal bone. The impact forces were recorded with a load transducer (4.45 kN capacity, model AL311CV; Sensotec, Columbus, OH) mounted immediately behind the impact interface.

In this study, each skull was dropped only once with a predetermined amount of potential energy. After impact, the scalp and soft tissues of the skull were carefully removed. Each skull was visually inspected for fractures that were then documented with photographs. The periosteum and remaining soft tissues were then removed. The skulls were then processed using standard anthropological procedures to remove all remaining soft tissue. The remains were then allowed to air-dry. The length of all skull fractures was measured to the nearest millimeter using a soft, flexible measuring tape that contoured to the curvature of the skull. Complete fracture diagrams were manually constructed for each specimen.

A Geographic Information System (GIS) method of analysis was utilized to document the pattern of cranial fractures, as previously described in Powell et al. (21). The pattern of cranial fractures from each skull was constructed using a projected view of the right porcine skull with superimposed fracture configurations for each specimen. A second view of the posterior aspect of the cranium was also included to display potential bone fractures in the occipital bone, which were documented in Powell et al. (21). The porcine specimens were separated into two age groups (2–9 and 10–17 days). These groupings coincided with the ages in which Powell et al. (21) documented changes in the fracture patterns that seemed to parallel with changes in porcine growth and development. Fracture pattern data from Powell et al. (21) were revisited here to directly compare fracture pattern data from the dropped head experiments using the 2- to 9-day-old and 10- to 17-day-old age groups to data from the previous entrapped head experiments. The patterns of fracture were then traced into individual shape files (24). The GIS software overlaid fracture patterns on each cranium and generated a map of where fractures appeared most frequently. After each map was constructed, the GIS maps were used to compare the patterns of fracture produced in the free-fall head experiments to the entrapped head experiments at the same impact energy level that varied according to subject age.

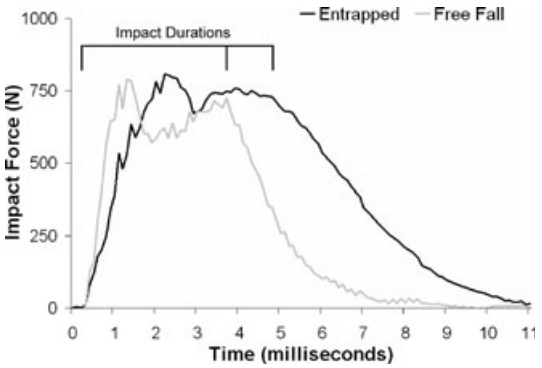


FIG. 4—*Typical plots of contact force versus time for free-fall and entrapped head experiments (from [21]).*

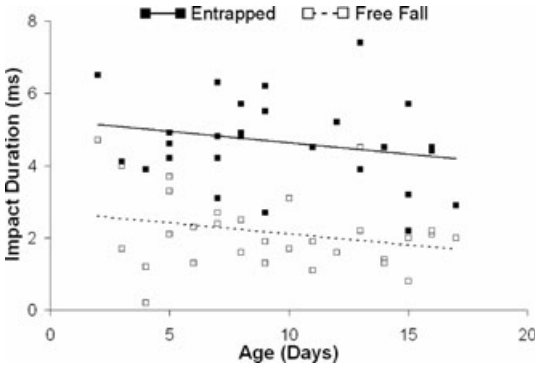


FIG. 5—*Impact duration with respect to age for free-fall and entrapped impacts.*

Impact force and total fracture length for the free-fall experiments were analyzed for age effects using linear regression analyses using commercial statistics software (SigmaStat 2.03; Aspire Software International, Ashburn, VA). A 2-factor (restraint condition, age) analysis of variance was performed for comparisons of peak impact forces, impact duration, and length of fracture between constraint conditions at each specimen age. Statistically significant effects were reported for $p$-values less than 0.05.

## Results

There was typically a characteristic rapid drop in impact force near the peak of the force–time plots, which was associated with skull fracture following examination of each specimen (Fig. 4).

Impact duration was defined as the time up to the point when the impact force began to decrease to zero. The impact duration was significantly shorter for the free-fall experiments than for the entrapped head experiments of Powell et al. (21) ($p < 0.001$) (Fig. 5).

On the other hand, the peak impact force data were not statistically different between the free-fall and entrapped head experiments of Powell et al. (21) (Fig. 6).

A comparison of the current data with Powell et al. (21) showed that there was significantly less skull fracture at each age for the free-fall experiments than for the entrapped head ($p < 0.001$) (Fig. 7). The total fracture length (bone and diastatic) also significantly decreased with age for the free-fall

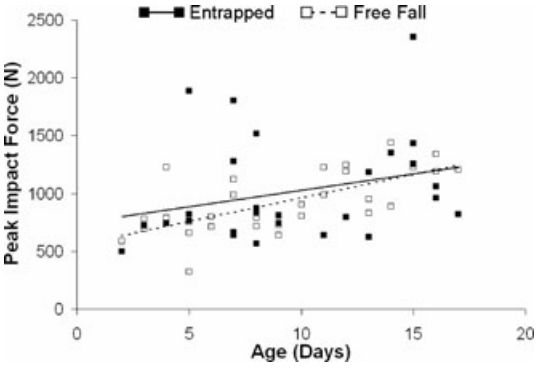


FIG. 6—*Peak impact force with respect to age for free-fall and entrapped impacts.*

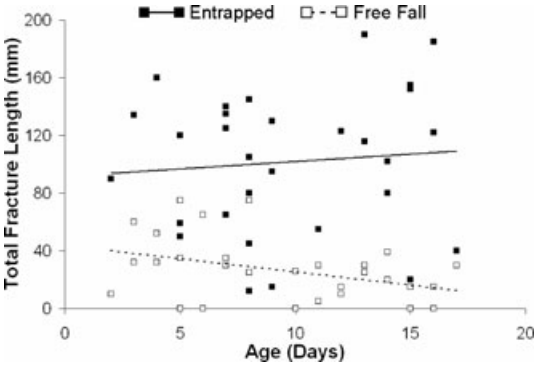


FIG. 7—*Total fracture (diastatic and bone) length with respect to specimen age for both impact scenarios.*

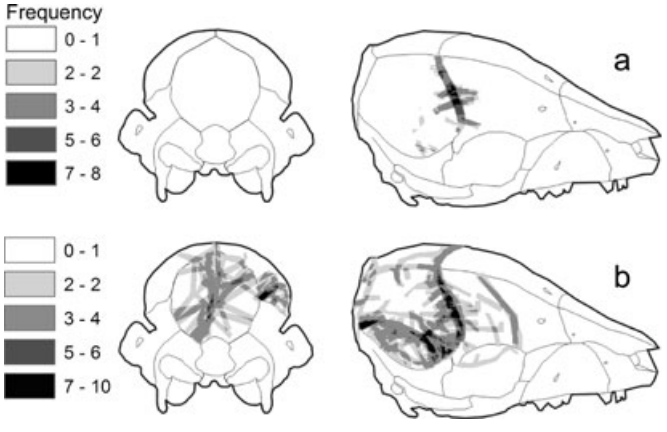


FIG. 8—*Geographic Information System (GIS) map of the 2- to 9-day-old age group for the free-fall (a) and entrapped (b) impacts, taken from revisited data from Powell et al. (21).*

experiments at a rate of approximately −1.83 mm/day ($p < 0.001$). In five of the 31 specimens, no cranial fractures (bone or diastatic) were documented.

In the young group of specimens (2–9 days old), extensive diastatic fracture was documented along the coronal suture in the free-fall experiments (Fig. 8*a*). Parietal bone fracture also typically initiated at the coronal suture, away from the point of impact. Additionally, several bilateral (occurring on both sides of the suture) bone fractures extended across the coronal suture into the frontal bone. There were no documented initiation sites

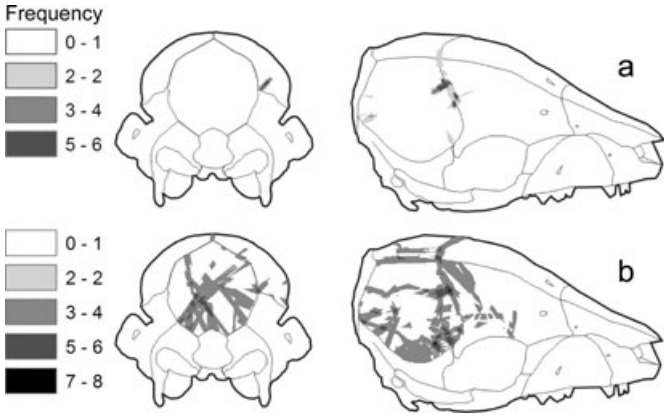


FIG. 9—*GIS map of the 10- to 17-day-old age group for the free-fall (a) and entrapped (b) impacts, taken from revisited data in Powell et al. (21).*

along the posterior or superior edges of the parietal bone in the free-fall experiments. There were also no occipital fractures in these free-fall head impacts. This contrasts with extensive occipital bone fractures in the revisited data from Powell et al. (21) (Fig. 8*a*).

In the older group of specimens (10–17 days old), several fracture initiation sites were noted near the intersection of the lambdoidal and squamosal sutures (Fig. 9*a*). However, fracture initiation was documented more frequently along the anterior parietal bone, as in the younger group of specimens. In contrast, the sites of fracture initiation were frequent and numerous around the entire perimeter of the parietal bone in Powell et al. (21) (Fig. 9*b*).

As in the young group of specimens, no occipital fractures were noted in the 10- to 17-day-old specimens when dropped in free fall. This again contrasted with extensive occipital fracture documented for the entrapped head impacts of Powell et al. (21). Diastatic fracture in the coronal suture was again noted in the older age group. However, the degree of diastatic fracture was significantly less for the older age group of specimens than for the younger aged group. Several of the older specimens also had fracture initiation sites on either side of the parietal bone at locations remote from the point of impact, as noted in Fig. 9*a*.

## Discussion

The objective of this study was to compare the fracture patterns on porcine skulls impacted once at the center of the parietal bone with a rigid interface at similar energy under free-fall and entrapped head restraint conditions. The results of the study showed that for the same level of impact force against the parietal bone, significantly less bone and diastatic fracture occurred under the free-fall than entrapped head condition. While in the entrapped head model, there were multiple cranial fractures in the parietal, occipital, and frontal bones, for the same impact energy in the free-fall experiments, fractures occurred in the parietal bone but often crossed the coronal suture into the frontal bone. The effect of crossing the coronal suture was more frequent in the younger (2–9 days of age) than older (10–17 days of age) group of specimens.

It is currently difficult to directly compare the results of this study with existing literature, as no studies on human or animal models have compared cranial fracture patterns on entrapped versus free-falling head models. It is interesting, however, that

the characteristic fracture patterns shown for the free-fall experiments on the developing porcine head do compare somewhat with the previous, lower energy experiments of Baumer et al. (19) using the same entrapped head model. Specifically, that study at one-half the impact energy of Powell et al. (21) documents parietal bone fracture initiation and propagation sites along the coronal and lambdoidal sutures in the parietal bone for the younger age group of specimens, which compared well to this study with the exception that fracture propagation often crossed the coronal suture into the frontal bone in the free-fall experiments. In the older age group of the Baumer et al.'s (19) study, fractures in the parietal bone were again located in the parietal bone, but there were also fractures produced in the occipital bone that were not observed in the older group of specimens in the free-fall experiments.

From a basic mechanics point of view, more extensive fracturing of cranial bone was expected in the entrapped than free-fall head experiments. Fracture is a process by which a material dissipates excess deformational energy under loading. Strictly speaking, with the entrapped head model, the cranial volume of material available to dissipate the energy of impact was limited by restraint offered by the head being mounted in a bed of epoxy. And thus, the state of bone stress was likely greater in the entrapped head experiments than in the free-fall experiments, which resulted in more extensive fracturing of the entrapped head. Fracture is known to be the key mechanic in maximizing energy dissipation in engineering materials (25). It is well known in the biomechanics literature that the extent of crack formation in engineering materials depends on the magnitude of the applied, dynamic stress field (26,27). Studies such as these have also shown that the duration of the applied stress field help determine the degree of crack formation in brittle materials. As noted in the current studies, the duration of impact loading on the entrapped skulls was shown to be significantly longer than on the free-fall heads, under the same level of impact energy and resultant impact force.

In a subsequent study by Powell (28), the entrapped and free-fall experiments were theoretically analyzed using a finite element modeling technique. The skull was modeled as an elastic shell using material properties from the literature (20,29) of mass 359 g, which was the average mass of a 2- to 9-day-old porcine head. The spherical skull was filled with a viscoelastic brain tissue with properties from the literature (30). Automatic surface-to-surface contact in LS-DYNA (Livermore Software Technology Corporation, Livermore, CA) with no penalty stiffness was used to define interaction between the impact interface (rigid) and the spherical head model. In the case of the entrapped head, large tensile stresses were developed in the spherical shell near the locations of constraint in the epoxy resin. This resulted in a "ballooning out" effect that could help explain the appearance of cranial fractures away from the site of impact in the center of the parietal bone and into the occipital bone. This effect may be similar to the so-called out-bending deformation pattern documented in free-fall drop tests using human heads (31–34). In contrast, the simulation of the free-falling head during contact with a rigid interface indicated tensile stress patterns in the shell located closer to the point of contact with the rigid interface, which may help explain the lack of occipital bone fracture in the free-fall experiments. A limitation of these studies was the simplification of the porcine head anatomy and material properties of the cranial bone and brain tissues, as well as the lack of sutures in the model. It is currently unclear what effect these limitations may play in helping to explain the differences in fracture patterns seen in these experiments with the entrapped and free-falling porcine head. In addition, to more completely compare responses of a fall victim to a victim lying against a rigid surface, whole-body kinematics and the potential for impact force dissipation through the body musculature will need to be considered (16). On the other hand, the current study focused directly on comparisons of the cranial fracture patterns of the free-falling porcine head to the constrained head for the same impact energy and force delivered to the subject head itself.

In summary, this study showed that physical restraint of the head during a blunt force impact generates relatively more cranial fractures than an impact that occurs during a free fall of the same magnitude of contact force and impact energy to the head. While there were some comparative results on the patterns of cranial fracture on the impacted bone that can be made between the free-fall experiment and a lower energy entrapped head situation, entrapment of the head can generate areas of high tensile stresses that may lead to bone fractures remote from the site of impact and near the area of physical restraint. The study on this developing porcine model also suggests that while impact force and energy are important factors determining the extent of cranial fracture, based on previous data by Baumer et al. (19) and Powell et al. (21), the level of head restraint during blunt force impacts needs to be considered in the determination of causal effects with respect to the distribution and extent of cranial fracture. While this study has been conducted on a porcine model, it may have direct utility in helping to guide future laboratory experiments using the human infant cadaver head and the interpretation of cranial fracture data in forensic case studies.

*Acknowledgments*

The authors would like to acknowledge Mr. Ed Reed and Ms. Star Lewis (Reed McKenzie Farms, Decatur, MI) for supplying and collecting the porcine specimens and Mr. Cliff Beckett for his technical support.

## References

1. Tabatabaei SM, Sedighi A. Pediatric head injury. Iranian J Child Neurology 2008;2(2):7–13.
2. Case ME, Graham MA, Handy TC, Jentzen JM, Monteleone JA. Position paper on fatal abusive head injuries in infants and young children. Am J Forensic Med Pathol 2001;22:112–22.
3. Zimmerman RA, Bilaniuk LT. Pediatric head trauma. Neuroimaging Clin N Am 1994;4(2):349–66.
4. Mayr JM, Seebacher U, Schimpl G, Fiala F. Highchair accidents. Acta Paediatr 1999;88:319–22.
5. Hall JR, Reyes HM, Horvat M, Meller JL, Stein R. The mortality of childhood falls. J Trauma 1989;29:1273–5.
6. Coats B, Margulies SS. Potential for head injuries in infants from low-height fall: laboratory investigation. J Neurosurg Pediatr 2008;2:321–30.
7. Hobb CJ. Skull fracture and the diagnosis of abuse. Arch Dis Child 1984;59:246–52.
8. Meservy CJ, Towbin R, McLaurin RL, Myers PA, Ball W. Radiographic characteristics of skull fractures resulting from child abuse. AJR Am J Roentgenol 1987;149:173–5.
9. Leventhal JM, Thomas SA, Rosenfield NS, Markowitz RI. Fracture in young children: distinguishing child abuse from unintentional injuries. Am J Dis Child 1993;147(1):87–92.
10. Billmire ME, Myers PA. Serious head injury in infants: accident or abuse? Pediatrics 1985;75:340–2.
11. Reece RM, Sege R. Childhood head injuries: accidental or inflicted. Arch Pediatr Adolesc Med 2000;154:11–5.
12. Wheeler DS, Shope TR. Depressed skull fracture in a 7-month old who fell from bed. Pediatrics 1997;100:1033–4.

13. Weber W. Experimental studies of skull fractures in infants. J Leg Med 1984;92(2):87–94.
14. Weber W. Biomechanical fragility of the infant skull. J Leg Med 1985;94(2):93–101.
15. Bertocci G, Pierce M. Applications of biomechanics aiding in the diagnosis of child abuse. Clin Pediatr Emerg Med 2006;7:194–9.
16. Snyder RG. Human tolerances to extreme impacts in free-fall. Aerosp Med 1963;36(10):695–709.
17. Herring S, Teng S. Strain in the braincase and its sutures during function. Am J Phys Anthropol 2000;112:575–93.
18. Pierce M, Valdevit A, Anderson L, Inoue N, Hauser D. Biomechanical evaluation of dual-energy x-ray absorptiometry for predicting fracture loads of the infant femur for injury investigation: an in vitro porcine model. J Orthop Trauma 2000;14(8):571–6.
19. Baumer TG, Passalacqua NV, Powell BJ, Newberry WN, Fenton TW, Haut RC. Age-dependent fracture characteristics of rigid and compliant surface impacts on the infant skull – a porcine model. J Forensic Sci 2010;55(4):993–7.
20. Baumer TG, Powell BJ, Fenton TW, Haut RC. Age dependent mechanical properties of the infant porcine parietal bone and a correlation to the human. J Biomech Eng 2009;131(11):1–6.
21. Powell B, Passalacqua N, Baumer T, Fenton T, Haut R. Fracture patterns on the infant porcine skull following severe blunt impact. J Forensic Sci 2012;57(2):312–7.
22. Fenton TW, DeJong JL, Haut RC. One unlucky blow: the etiology of a depressed skull fracture. J Forensic Sci 2003;48(2):277–81.
23. Chason JL, Fernando OU, Hodgson VR, Thomas LM, Gurdjian ES. Experimental brain concussion: morphologic findings and a new cytologic hypothesis. J Trauma 1966;6(6):767–79.
24. Marean CW, Abe Y, Nilssen PJ, Stone EC. Estimating the minimum number of skeletal elements (MNE) in zooarchaeology: a review and a new image-analysis GIS approach. Am Antiq 2001;66(2):333–48.
25. Frank F, Lawn B. On the theory of hertzian fracture. Proc R Soc Lond 1967;299(1458):291–306.
26. Evans AG, Gulden ME, Rosenblatt M. Impact damage in brittle materials in the elastic-plastic response régime. Proc R Soc Lond 1978;A361:343–65.
27. Seaman L, Curran DR, Shockey DA. Computational models for ductile and brittle fracture. J Applied Physics 1976;47(11):4814–26.
28. Powell BS. Fracture patterns of the developing skull attributable to different impact scenarios [MS Thesis]. East Lansing (MI): Michigan State University, 2010.
29. Margulies SS, Thibault KL. Infant skull and suture properties: measurements and implications for mechanisms of pediatric brain injury. J Biomech Eng 2000;122(4):364–71.
30. Mao H, Zhang L, Yang K, King A. Application of a finite element model of the brain to study traumatic brain injury mechanisms in the rat. Stapp Car Crash J 2006;50:583–600.
31. Gurdjian ES, Lissner HR. Deformation of the skull in head injury; a study with the stress coat technique. Surg Gynecol Obstet 1945;81:679–87.
32. Gurdjian ES, Webster JE, Lissner HR. The mechanism of production of linear skull fractures. Surg Gynecol Obstet 1947;85:195–210.
33. Gurdjian ES, Webster JE, Lissner HR. The mechanism of skull fracture. Radiology 1950;54(3):313–39.
34. Gurdjian ES, Webster JE, Lissner HR. The mechanism of skull fracture. J Neurosurg 1950;2:106–14.

Additional information and reprint requests:
Roger C. Haut, Ph.D.
Orthopaedic Biomechanics Laboratories
A-407 East Fee Hall
Michigan State University
East Lansing, MI 48824
E-mail: haut@msu.edu